First principles investigations on elastic and electronic properties of BaHfN$_2$ under pressure

Peng Wang[a], Yan Cheng[a,*], Xu-Hui Zhu[a], Xiang-Rong Chen[a,b,**], Guang-Fu Ji[c]

[a] College of Physical Science and Technology, Sichuan University, Chengdu 610064, China
[b] International Centre for Materials Physics, Chinese Academy of Sciences, Shenyang 110016, China
[c] National Key Laboratory for Shock Wave and Detonation Physics Research, Institute of Fluid Physics, Chinese Academy of Engineering Physics, Mianyang 621900, China

ARTICLE INFO

ABSTRACT

We investigate the elastic and electronic structure properties of BaHfN$_2$ under pressure by performing the generalized gradient approximation (GGA) and local density approximation (LDA) correction scheme in the frame of density functional theory (DFT). The pressure dependences of the normalized lattice parameters a/a_0 and c/c_0, the ratio c/a, and the normalized primitive volume V/V_0 of BaHfN$_2$ are also obtained. The obtained lattice constants and bulk modulus agree well with the available experimental and other theoretical data. The pressure dependences of elastic properties are investigated for the first time. It is found that, as the pressure increases, the elastic constants C_{11}, C_{33}, C_{66}, C_{12} and C_{13} increase, the variation of elastic constant C_{44} is not obvious. At 40 GPa, the tetragonal structure BaHfN$_2$ transfers to another structure at zero temperature. Moreover, our compressional and shear wave velocities $V_L = 5.87$ km/s and $V_S = 3.12$ km/s as well as the Debye temperature $\Theta = 451.7$ K at 0 GPa are obtained. The pressure dependences of the band structures, energy gap and density of states are also investigated.

1. Introduction

In the last few decades, metal–nitrides have attracted a lot of attention for its important properties including superconductivity, catalytic activity, unusual magnetic and mechanical properties [1–7]. Many researchers have spent a lot of time to investigate and synthesis the binary metal-nitride films, such as Hf$_3$N$_2$, Cu$_3$N and CaN, by metalorganic chemical vapor deposition (MOCVD) and molecular-beam epitaxy (MBE) [8–10]. However, when they further get the single crystal of those ternary and multiple-nitrides, those methods are not suitable. Hence, they only predict the related properties of the pure crystal through the test of the materials doped. Recently, in order to validate the predicted result is correct or not, Luo et al. [11,12] obtained the single crystals by polymer-assisted deposition (PAD) method [13,14]. In addition, they found that both BaZrN$_2$ and BaHfN$_2$ show metallic-like resistivity-temperature behavior from 5 to 300 K with RRRs ($\rho_{300 K}/\rho_{5 K}$) as large as 396 and 203, respectively. The inner physical properties of those materials have not been researched yet.

Hence, it gives us the chance to make a further research for those kinds of materials.

Up to date, there have been many scientific investigations on AMN$_n$ (where A = alkali metal, alkaline earth metal, or transition metal; M = transition metal or lanthanide) on several aspects. For examples, the synthesis of AMN$_3$ by Brese and Disalvo [15] and DiSalvo and Clarke [3], the synthesis, structure and magnetic properties of SrZrN$_2$, SrHfN$_2$, SrTiN$_2$, BaHfN$_2$ and the BaHf$_{1-x}$Zr$_x$N$_2$ solid solution by Gregory et al. [16–19] and Sr$_2$NbN$_3$, BaThN$_2$ by Chen et al. [20], a new PAD method to obtained ternary nitrides by Luo et al. [11,12], the electronic and vibrational properties of BaHfN$_2$ by Kaur et al. [21]. However, there are little reports on the inner properties of AMN$_2$ under pressure.

In this work, we focus on the ternary nitride BaHfN$_2$, whose elastic properties have not yet been studied. BaHfN$_2$ has many chemical and structural similarities with the layered transition-metal nitrides MNCl's (M = Ti, Hf, Zr) that are impressive superconductors when they are electron doped. The BaHfN$_2$ crystal belongs to the tetragonal space group $P4/nmm$ ($a = 4.1279$ Å and $c = 8.3816$ Å). The structural coordinates of BaHfN$_2$ are known from powder X-ray diffraction reported by Gregory et al. [19]. In Section 2, the theoretical method is introduced and the computation details are given. Some results and discussion are presented in Section 3. Finally, the summary of our main results is given in Section 4.

* Corresponding author. Tel.: +86 28 85405516.
** Corresponding author at: College of Physical Science and Technology, Sichuan University, Chengdu 610064, China. Tel.: +86 28 85405516.
E-mail addresses: ycheng@scu.edu.cn (Y. Cheng), x.r.chen@qq.com (X.-R. Chen).

2. Theoretical method and computation details

2.1. Total energy electronic structure calculations

In our electronic structure calculations, for the primitive unit cell of $BaHfN_2$, we employ three pseudopotentials, i.e. the norm-conserving (NC), ultrasoft, and on-the-fly (OTF), for the interactions of the electrons with the ion cores, respectively, together with the generalized gradient approximation (GGA) proposed by Perdew and Wang [22] and the local density approximation (LDA) proposed by Vosko et al. [23] for exchange-correlation potential. We have made some convergence tests to the unit cell size and obtain those parameters as follows. The electronic wave functions are expanded in a plane wave basis set with energy cut-off of 600 eV with LDA and 450 eV with GGA. The atomic levels $5s^2 5p^6 6s^2$ of Ba atom, $5d^2 6s^2$ of Hf atom, and $2s^2 2p^3$ of N atom were treated as valence electron states. For the Brillouin-zone sampling, we use the $5 \times 5 \times 3$ and $6 \times 6 \times 3$ Monkhorst–Pack mesh [24] for LDA and GGA, respectively. The self-consistent convergence of the total energy is 10^{-6} eV/Atom, the maximum ionic Hellmann–Feynman force within 0.05 eV/Å, the maximum ionic displacement within 0.002 Å, and the maximum stress within 0.1 GPa. These parameters are carefully tested. It is found that these parameters are sufficient to lead to a well-converged total energy. All these electronic structure calculations are implemented through the CASTEP code [25,26].

The pressure–volume relationship can be obtained by fitting the calculated energy–volume (E–V) data to the Vinet EOS [27],

$$\ln\left(\frac{Px^2}{3(1-x)}\right) = \ln B_0 + a(1-x), \quad x = \left(\frac{V}{V_0}\right)^{1/3} \tag{1}$$

where $V = V(0,T)$ is the zero-pressure equilibrium volume, derived by integration of the thermodynamic definition of the thermal expansion coefficient $\alpha(T) = V^{-1}(\partial V/\partial T)$

$$V(0,T) = V(0,0)\exp\int_0^T \alpha(T)\,dT \tag{2}$$

B_0 and a $(= 3(B_0' - 1)/2)$ are the fitting parameters. $B_T(P,T)$, $B_T'(P,T)$, and $B_T''(P,T)$ are given by:

$$B_T = -x^2 B_0\, e^{\alpha(1-x)} f(x) \tag{3}$$

$$B_T' = \left(\frac{\partial B_T}{\partial P}\right)_T = \frac{1}{3}\left[(ax + 2) - x\frac{f'(x)}{f(x)}\right] \tag{4}$$

$$B_T'' = \left(\frac{\partial^2 B_T}{\partial P^2}\right)_T = \frac{x}{9B_T}\left\{x\frac{f''(x)}{f(x)} - a + \frac{f'(x)}{f(x)}\left[1 - x\frac{f''(x)}{f(x)}\right]\right\} \tag{5}$$

where $f(x) = x - 2 - ax(1-x)$.

2.2. Elastic properties and Debye temperature

To calculate the elastic constants under hydrostatic pressure P, we use the symmetry-dependent strains that are non-volume conserving. The elastic constants, C_{ijkl}, with respect to the finite strain variables is defined as [28]:

$$C_{ijkl} = \left(\frac{\partial \sigma_{ij}(x)}{\partial e_{kl}}\right)_X \tag{6}$$

where σ_{ij} and e_{kl} are the applied stress and Eulerian strain tensors, X and x are the coordinates before and after deformation, respectively. Under the hydrostatic pressure P,

$$C_{ijkl} = c_{ijkl} + \frac{p}{2}(2\delta_{ij}\delta_{kl} - \delta_{il}\delta_{jk} - \delta_{ik}\delta_{jl}) \tag{7}$$

where c_{ijkl} denotes the second-order derivatives with respect to the infinitesimal strain (Eulerian), δ is the finite strain variable. The fourth-rank tensor C generally greatly reduces when taking into account the symmetry of the crystal. Since the stress and strain tensors are symmetric, the most general elastic stiffness tensor has only 21 non-zero independent components. For the tetragonal $BaHfN_2$ crystal, it is reduced to six components, i.e. C_{11}, C_{33}, C_{44}, C_{66}, C_{12}, and C_{13}.

The Debye temperature may be estimated from the average sound velocity V_m [29],

$$\Theta = \frac{\hbar}{k}\left[\frac{3n}{4\pi}\left(\frac{N_A \rho}{M}\right)\right]^{1/3} V_m \tag{8}$$

where $\hbar$ is the Planck's constants, k is the Boltzmann's constant, N_A is the Avogadro's number, n is the number of atoms per formula unit, M is the molecular mass per formula unit, $\rho(= M/V)$ is the density, and V_m is obtained from,

$$V_m = \left[\frac{1}{3}\left(\frac{2}{V_S^3} + \frac{1}{V_L^3}\right)\right]^{-1/3} \tag{9}$$

where V_S and V_L are the shear and longitudinal sound velocities, respectively.

According to the Voigt approximation [30], there is a simple relation between the isotropic bulk moduli B_V and shear moduli G_V of a polycrystalline aggregate and the single-crystal elastic constants C_{ij},

$$B_V = \frac{1}{9}[2(C_{11} + C_{12}) + C_{33} + 4C_{13}] \tag{10a}$$

$$G_V = \frac{1}{15}(2C_{11} - C_{12} + C_{33} - 2C_{13} + 6C_{44} + 3C_{66}) \tag{10b}$$

Reuss [31] derived a linear relation between the isotropic bulk B_R and shear moduli G_R of a polycrystalline aggregate, and the corresponding sing-crystal elastic constants S_{ij},

$$B_R = \frac{1}{2S_{11} + S_{33} + 2S_{12} + 4S_{13}} \tag{11a}$$

$$G_R = \frac{15}{8S_{11} + 4S_{33} - 4S_{12} - 8S_{13} + 6S_{44} + 3S_{66}} \tag{11b}$$

For $BaHfN_2$ crystal, we can obtain the relations between C_{ij} and S_{ij} as follows:

$$S_{11} = \frac{C_{33}C_{11} - 2C_{33}^2}{(C_{11} - C_{12})[C_{33}(C_{11} + C_{12}) - 2C_{13}^2]} \tag{12}$$

$$S_{12} = \frac{C_{13}^2 - C_{33}C_{12}}{(C_{11} - C_{12})[C_{33}(C_{11} + C_{12}) - 2C_{13}^2]} \tag{13}$$

$$S_{13} = -\frac{C_{13}}{C_{33}(C_{11} + C_{12}) - 2C_{13}^2} \tag{14}$$

$$S_{33} = \frac{C_{11} + C_{12}}{C_{33}(C_{11} + C_{12}) - 2C_{13}^2} \tag{15}$$

$$S_{44} = \frac{1}{C_{44}} \tag{16}$$

$$S_{66} = \frac{1}{C_{66}} \tag{17}$$

Hill [32] proved that the Voigt and Reuss equations represent upper and lower limits of the true polycrystalline constants. He showed that the polycrystalline moduli are the arithmetic mean values of the Voigt and Reuss moduli and thus given by:

$$G_H = \frac{1}{2}(G_R + G_V), \qquad B_H = \frac{1}{2}(B_R + B_V) \tag{18}$$

The probable values of the average shear and longitudinal sound velocities can be calculated from Hill's equations as follows:

$$V_S = \sqrt{\frac{G_H}{\rho}}, \qquad V_L = \sqrt{\frac{(B_H + (4/3)G_H)}{\rho}} \tag{19}$$

By applying the method, we have investigated successfully the elastic properties of several materials, such as CoVSb, Zr_2Al, BC_2N, and LiZnN [33–36].

3. Results and discussion

For the tetragonal structure $BaHfN_2$, the initial structural model is built according to previous available lattice parameters a and c. In its unit cell, there are two inequivalent N sites which we expressed as N_I (lying nearly in the Hf plane) and N_{II} (nearly in the Ba plane), i.e. BaN_{II}–HfN_I. The atom of Ba is set at position $(0.25, 0.25, z_1)$, the two N atoms at positions $(0.75, 0.25, 0.5)$ and $(0.25, 0.25, z_2)$, and the Hf atom at position $(0.25, 0.25, z_3)$. We optimized the lattice geometry to get a fully stable structure of $BaHfN_2$. In the equilibrium geometry calculations, we performed the following procedures: firstly, for a fixed axial ratio c/a, we take a series of different values of a and c to calculate the total energies E and the corresponding primitive cell volumes V, and then obtain the lowest energy E_{min} for the given ratio c/a. This procedure is repeated over a wide range of c/a. Finally, we obtained the equilibrium parameters a, c, and c/a of $BaHfN_2$.

In Table 1, we list our results together with the available experimental data and other theoretical results. Obviously, our results from GGA–OTF and LDA–ultrasoft are better than other pseudopotentials (PSPs) for both GGA and LDA methods. The equilibrium unit cell volume calculated by GGA–OTF is less than the experimental value with the error of 0.9%, which leads to a lower B_0 directly. We made the GGA calculations with three PSPs of NC, ultrasoft and OTF, respectively, and obtain the results with the errors: 1.7%, 2.5%, 0.6% for lattice constant a, and 3.1%, 1.5%, 0.4% for lattice constant c, respectively. But as for the LDA calculations, the corresponding

Table 1
Structurally optimized lattice constants (a and c), the band gap E_g^{exp} and reduced internal coordinates (z) for atoms in the unit cell, together with the experimental data and other theoretical results obtained from different sets of pseudopotentials (PSPs) including Hartwigsen–Goedecker–Hutter (HGH) and Troullier–Martin (TM) type.

	Method	PSP	a/a_{exp}	c/c_{exp}	z (Ba)	z (Hf)	z (N$_2$)	B_0	B_0'	E_g^{exp} (eV)
This work	PBE	OTF	1.006	0.996	0.8479	0.414	0.168	136.42	4.7311	0.768
		Ultrasoft	1.025	1.015	0.8489	0.413	0.170	129.12	4.538	1.013
	LDA	NC	0.983	0.969	0.8467	0.4167	0.184	140.94	4.19	1.265
		OTF	0.992	0.973	0.8450	0.4167	0.175	155.58	4.4688	0.606
		Ultrasoft	1.009	0.994	0.8479	0.414	0.168	148.64	4.4627	0.691
		NC	0.982	0.953	0.8478	0.4152	0.178	149.48	4.1733	0.977
Cal. [21]	PBE	HGH, Ba^{sc}, Hf^{sc}	1.000	1.007	0.848	0.415	0.180			0.95
		TM	1.022	1.036	0.845	0.416	0.186			1.00
	LDA	TM, Ba^{sc}	1.011	1.008	0.850	0.413	0.175			1.13
		TM, Ba^{sc}, Hf^{sc}	1.004	0.999	0.849	0.414	0.179			1.25
		FPLO	0.992	0.986	0.846	0.415	0.177			0.68
		FLAPW								0.8
		HGH, Ba^{sc}, Hf^{sc}	0.986	0.982	0.848	0.415	0.176			0.82
		TM	1.005	1.017	0.846	0.415	0.177			0.78
		TM, Ba^{sc}	0.997	0.987	0.849	0.413	0.170			0.87
		TM, Ba^{sc}, Hf^{sc}	0.984	0.972	0.847	0.415	0.177			1.11
Exp. [19]					0.8479	0.4142	0.168			

errors are 1.8%, 0.9%, 0.8% for a, and 4.7%, 0.6%, 2.7% for c, respectively. It is seen that the results from GGA–OTF seem to be the best. In addition, when compared with other results, our results calculated with GGA–OTF are in good agreement with those calculated by Kaur et al. [21] with PBE (Hartwigsen–Goedecker–Hutter, Ba^{sc}, Hf^{sc}) and seem to be best than the data obtained with other PSPs.

We also obtained the crystal coordinates z_1, z_2 and z_3, which agree well with the results by Gregory et al. [19] and Kaur et al. [21]. The obtained bulk modulus B_0 and its pressure derivative B_0, with GGA and LDA calculations are also listed in Table 1. Unfortunately, there are no experimental and other theoretical data for our comparison. It is instructive for future studies to quantify the effects of different types of PSPs on the relaxed structure and the energy gap [21]. Here, we have investigated the BaHfN$_2$ crystal by using both GGA (with NC, ultrasoft and OTF pseudopotentials) and LDA (with NC, ultrasoft and OTF pseudopotentials). In Table 1, the results are listed and compared with other theoretical values [21]. It is shown that the data we obtained by GGA(LDA) are 0.768 (0.606) eV (OTF), 1.013(0.691) eV (ultrasoft), 1.265 (0.977) eV (NC), which are agreement with the results 0.95 (0.82) eV (HGH, Ba^{sc}, Hf^{sc}), 1.00 (0.78) eV (TM), 1.13 (0.87) eV (TM, Ba^{sc}), 1.25 (1.11) eV (TM, Ba^{sc}, Hf^{sc}) obtained with GGA (LDA) by Kaur et al. [21]. Thus, the results obtained by us should be reliable. Since GGA–OTF seems to be best, we just apply them in the following calculations.

In Fig. 1, we illustrated the pressure dependences of the normalized lattice constants a/a_0, c/c_0, and the normalized cell volume V/V_0 of BaHfN$_2$, where a_0, c_0 and V_0 are the zero pressure equilibrium structure parameters. From Fig. 1, we can see that the changes of the ratios of a/c keep constant with the pressure change for both GGA–OTF, roughly. As the applied pressure increases from 0 to 20 GPa (4, 8, 12, 16, 20 GPa), the ratio c/c_0 decreases more quickly 1.234%, 0.982%, 0.67%, 0.623%, 0.527% than a/a_0 0.722%, 0.722%, 0.747%, 0.674%, 0.626%, respectively, indicating that the compression along c-axis is larger. Also, there have a big kick point when we add the pressure up to 4 GPa for lattice constant a.

In Table 2, we present our calculated elastic constants (C_{11}, C_{12}, C_{13}, C_{33}, C_{44} and C_{66}) and aggregate elastic modulus B, shear modulus G, B/G, the compressional and shear wave velocities, elastic Debye temperature Θ of the structure BaHfN$_2$ at 0 K and pressure range 0–20 GPa. Similarly, no experimental and theoretical data of elastic constants are available for us to compare with. It is shown that the elastic constants C_{11}, C_{33}, C_{66}, C_{12} and C_{13} increase with the increasing pressure, while C_{44} increases slowly with the elevated pressure but fluctuates inconspicuously at higher pressure. From Eq. (18), the bulk modulus B (in Table 2) obtained by our elastic
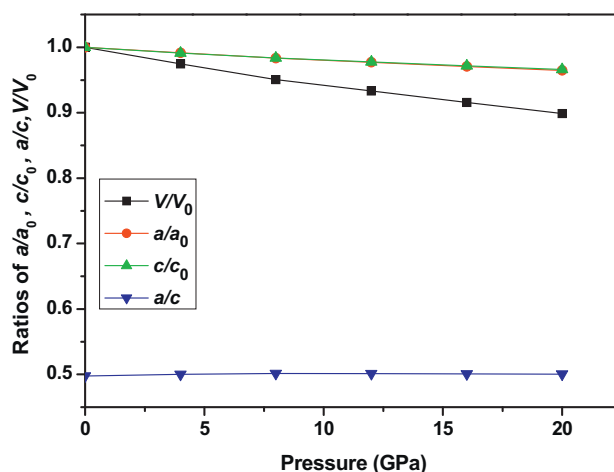
Fig. 1. The normalized parameters a/a_0, c/c_0, a/c and V/V_0 of BaHfN$_2$ as a function of pressure at $T = 0$ from GGA–OTF.

constants is 119.64 GPa for GGA–OTF, which consist with the value (in Table 1) estimated by fitting the E–V data mentioned in Ref. [27].

The mechanical stability conditions in the tetragonal structures can be expressed in terms of elastic constants as follows [37]: ($\tilde{C}_{11}$ + $\tilde{C}_{33} - 2\tilde{C}_{13}$) > 0, $\tilde{C}_{11} > 0$, $\tilde{C}_{33} > 0$, $\tilde{C}_{44} > 0$, $\tilde{C}_{66} > 0$, $\tilde{C}_{11} - \tilde{C}_{12} >$ 0, ($2\tilde{C}_{11} + 2\tilde{C}_{12} + \tilde{C}_{33} + 4\tilde{C}_{13}$) > 0, where $\tilde{C}_{\alpha\alpha} = C_{\alpha\alpha} - P$ ($\alpha = 1, 3, 4, 6$), $\tilde{C}_{12} = C_{12} + P$, $\tilde{C}_{13} = C_{13} + P$. It is obvious from Table 2 that the elastic constants of BaHfN$_2$ satisfy all of these conditions above at

Table 2
Calculated elastic constants C_{ij} (GPa), bulk modulus B (GPa), shear modulus G (GPa), B/G, acoustic velocities V_L and V_S (km/s), and Debye temperature Θ (K) of BaHfN$_2$ under pressure up to 20 GPa from GGA–OTF.

P	0	4	8	12	16	20
C_{11}	196.0	204.8	226.7	236.2	243.8	245.8
C_{33}	153.2	165.2	192.2	225.1	236.2	237.0
C_{44}	46.5	47.2	50.1	50.1	45.8	49.6
C_{66}	106.1	112.8	119.2	125.3	131.1	136.7
C_{12}	128.7	149.0	171.5	187.4	213.4	225.9
C_{13}	75.5	97.8	91.4	93.6	117.5	124.0
B	119.64	137.32	146.97	158.31	177.48	183.22
G	53.45	51.41	56.74	58.01	50.55	47.53
B/G	2.24	2.67	2.59	2.73	3.51	3.85
V_L	5.87	6.02	6.18	6.29	6.35	6.31
V_S	3.12	3.01	3.12	3.12	2.88	2.77
Θ	451.70	442.62	462.82	466.72	436.15	422.27

Table 3
Elastic constants C_{ij} (GPa) of BaHfN$_2$ under pressure from GGA-OTF.

P	0	20	40	60
C_{11}	196	245	308	361
C_{33}	153	237	407	504
C_{44}	46	49	23	−72
C_{66}	106	136	165	182
C_{12}	128	225	335	411
C_{13}	75	124	178	289

pressure P below 20 GPa. In order to further study, we try to add up to 60 GPa (in Table 3), and found that when $P > 40$ GPa, $\tilde{C}_{44} < 0$, it suggests that its structure phase transition of BaHfN$_2$ may be happened. For $C_{44} = -72$ GPa, we can judge that the structure of this material is not stable at 60 GPa. According to the elastic constants obtained, we can also obtain the compressional and shear wave velocities of BaHfN$_2$ under pressure. We list them in Table 2, the results of them are $V_L = 5.87$ km/s and $V_S = 3.12$ km/s at 0 GPa with GGA–OTF. It is shown that (in Fig. 2) with the pressure increasing, the compressional wave velocities increases first, then gently. The shear wave velocity changes slowly with the elevated pressure, but fluctuates inconspicuously at higher pressure.

It is acknowledged that the bulk modulus or shear modulus can measure the hardness in an indirect way [38]. From Table 2, we can find that the bulk modulus B increases gradually with the increase of pressure, indicating that the tetragonal structure BaHfN$_2$ becomes more difficult to compress with the increasing pressure. Obviously, the volume will change greatly. We can predict the volume change results in rapidly change in the bulk modulus. Pugh indicated that a material is breakable if the B/G ratio is less than 1.75 [39]. In our work, the B/G ratio of BaHfN$_2$ is 2.24 for GGA–OTF at 0 GPa, hence describing the structure of this material as ductile. The B/G ratio increases with the increasing pressure, suggesting that it becomes much harder with the pressure increases. The Debye temperature is an important parameter related to many physical properties of solids, such as specific heat, elastic constants, and melting temperature. From the calculated Debye temperature in Table 2, we can clearly see that the Debye temperatures increase with the increasing pressure.

The density of states (DOS) plays an important role in the analysis of the physical properties of materials. Here, we perform an analysis of the changes in the DOS of BaHfN$_2$ under different pressures with GGA–OTF. The total density of states (TDOS) and partial density of states (PDOS) are illustrated in Fig. 3. It is shown that, at
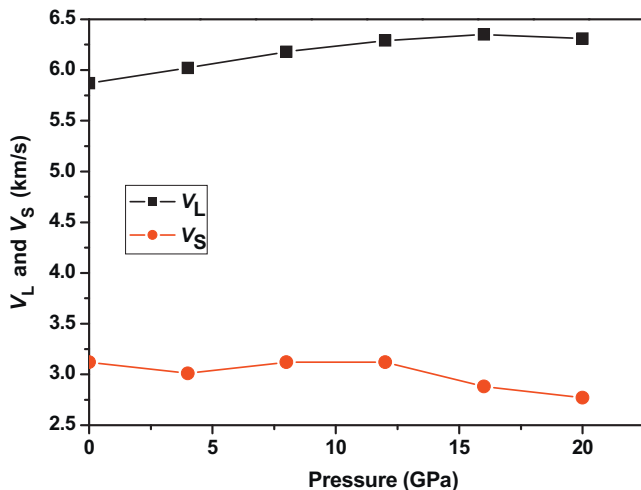
Fig. 2. The compressional and shear wave velocities of BaHfN$_2$ as a function of pressure at $T = 0$ from GGA–OTF.
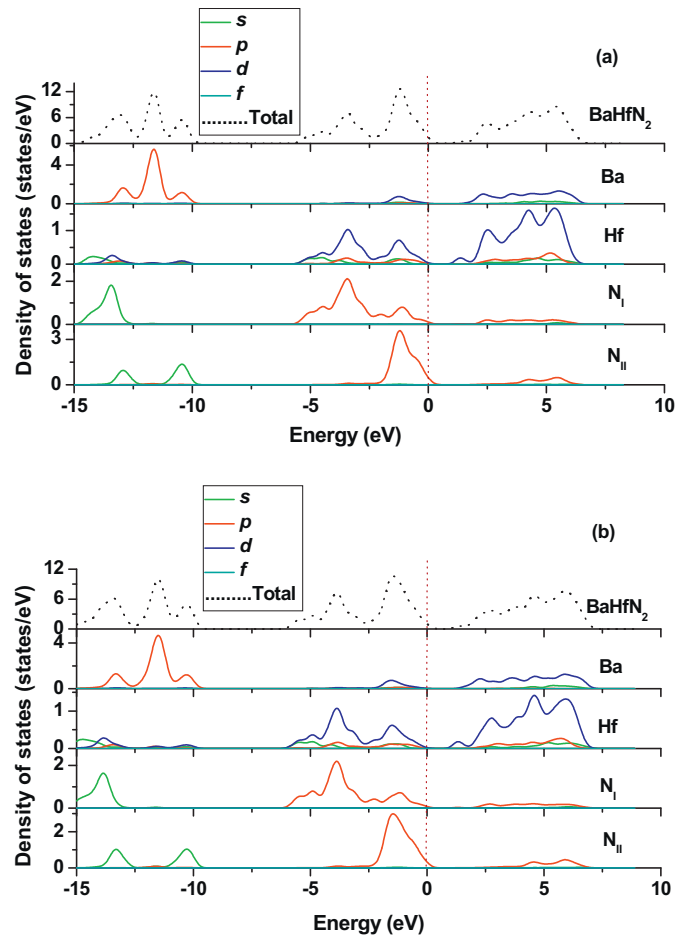
Fig. 3. Total density of states (TDOS) and partial density of states (PDOS) of BaHfN$_2$ under pressure from GGA–OTF calculations: (a) 0 GPa, (b) 20 GPa.

0 GPa, the high DOS about −2.5 eV to −1 eV is owing to 2p bands of N$_{II}$ atoms and the second-high DOS about −5 eV to −2.5 eV is owing to Hf-5d and N$_I$-2p; at high pressure, the DOSs of Ba, Hf and N atoms get reduced at E_F, the DOS peak near Fermi level E_F moves slowly away from it. The lowest valence bands are calculated in the energy range from −15 eV to −12 eV. These bands are essentially dominated by N$_I$-2s states with a minor presence of Ba-5p and Hf-5d states, especially, at the region closer to the E_F. The total DOS shows that BaHfN$_2$ has a pseudo-gap. The pseudo-gap of BaHfN$_2$ is below E_F and anti-bonding states are occupied. Furthermore, we investigate the variety tendency of the TDOS and PDOS at higher pressures. It is found that the TDOS values become smaller when the pressure is increased, especially the value in the range of conduction band, as well as the peak value of N$_{II}$-2p. Thus, we can predict that the obtained peak is due to N$_{II}$-2p and Hf-5d, which consist with the conclusions of Kaur et al. [21].

4. Conclusions

We have investigated the elastic and electronic structure properties of BaHfN$_2$ under pressure by performing the generalized gradient approximation (GGA) and local density approximation (LDA) correction scheme in the frame of density functional theory (DFT). The pressure dependences of the normalized lattice parameters a/a_0 and c/c_0, the ratio c/a, and the normalized primitive volume V/V_0 of BaHfN$_2$ are also obtained. The lattice constants and bulk modulus obtained here are in good agreement with the available experimental and other theoretical data. The pressure

dependences of elastic properties are investigated for the first time. It is found that, as pressure increases, the elastic constants C_{11}, C_{33}, C_{66}, C_{12} and C_{13} increase, the variation of elastic constant C_{44} is not obvious. At 40 GPa, the tetragonal structure BaHfN$_2$ may become another structure at zero temperature. Moreover, our compressional and shear wave velocities $V_L = 5.87$ km/s and $V_S = 3.12$ km/s as well as the Debye temperature $\Theta = 451.70$ K at 0 GPa are obtained for GGA–OTF. Finally, the pressure dependences of the band structures, energy gap and density of states are also investigated.

Acknowledgments

References

[1] F.J. Disalvo, Science 247 (1990) 649.
[2] N. Brese, M. O'Keeffe, Struct. Bond. 79 (1992) 307.
[3] F.J. DiSalvo, S.J. Clarke, Curr. Opin. Solid State Mater. Sci. 1 (1996) 241.
[4] R. Niewa, H. Jacobs, Chem. Rev. 96 (1996) 2053.
[5] M.A. Sriram, K.S. Weil, P.N. Kumta, Appl. Organometall. Chem. 11 (1997) 163.
[6] R. Kniep, Pure Appl. Chem. 69 (1997) 185.
[7] X.F. Li, Z.L. Liu, J. At. Mol. Sci. 3 (2012) 78.
[8] J.Y. Shi, L.P. Yu, Y.Z. Wang, G.Y. Zhang, H. Zhang, Appl. Phys. Lett. 80 (2002) 2293.
[9] J. Narayan, P. Pant, A. Chugh, H. Choi, J.C.C. Fan, J. Appl. Phys. 99 (2006) 054313.
[10] P.K. Kuo, G.W. Auner, Z.L. Wu, Thin Solid Films 253 (1994) 223.
[11] H.M. Luo, H.Y. Wang, Z.X. Bi, G.F. Zou, T. Mark McCleskey, A.K. Burrell, E. Bauer, M.E. Hawley, Y.Q. Wang, Q.X. Jia, Angew. Chem. Int. Ed. 48 (2009) 1490.
[12] H.M. Luo, H.Y. Wang, G.F. Zou, E. Bauer, T. Mark McCleskey, A.K. Burrell, Q.X. Jia, Trans. Electr. Electron. Mater. 11 (2010) 54.
[13] F.F. Lange, Science 273 (1996) 903.
[14] Q.X. Jia, T. Mark McCleskey, A.K. Burrell, Y. Lin, G.E. Collis, H. Wang, A.D.Q. Li, S.R. Foltyn, Nat. Mater. 3 (2004) 529.
[15] N.E. Brese, F.J. Disalvo, Solid State Chem. 120 (1995) 278.
[16] D.H. Gregory, M.G. Barker, P.P. Edwards, D.J. Siddons, Inorg. Chem. 35 (1996) 7608.
[17] D.H. Gregory, M.G. Barker, P.P. Edwards, D.J. Siddons, Inorg. Chem. 37 (1998) 3775.
[18] D.H. Gregory, P.M. O'Meara, A.G. Gordon, D.J. Siddons, A.J. Blake, M.G. Barker, T.A. Hamor, P.P. Edwards, J. Alloys Compd. 317–318 (2001) 237.
[19] D.H. Gregory, M.G. Barker, P.P. Edwards, M. Slaski, D.J. Siddons, Solid State Chem. 137 (1998) 62.
[20] X.Z. Chen, H.A. Eick, W. Lasocha, Solid State Chem. 138 (1998) 297.
[21] A. Kaur, E.R. Ylvsaker, Y. Li, G. Galli, W.E. Pickett, Phys. Rev. B 82 (2010) 155125.
[22] J.P. Perdew, Y. Wang, Phys. Rev. B 45 (1992) 13244.
[23] S.H. Vosko, L. Wilk, M. Nusair, Can. J. Phys. 58 (1980) 1200.
[24] H.J. Monkhorst, J.D. Pack, Phys. Rev. B 13 (1976) 5188.
[25] M.C. Payne, M.P. Teter, D.C. Allen, T.A. Arias, J.D. Joannopoulos, Rev. Mod. Phys. 64 (1992) 1045.
[26] V. Milan, B. Winker, J.A. White, C.J. Packard, M.C. Payne, E.V. Akhmatskaya, R.H. Nobes, Int. J. Quantum Chem. 77 (2000) 895.
[27] P. Vinet, J.H. Rose, J. Ferrante, J.R. Smith, J. Phys.: Condens. Matter 1 (1989) 1941.
[28] D.C. Wallace, Thermodynamics of Crystals, Wiley, New York, 1972.
[29] (a) O.L. Anderson, J. Phys. Chem. Solids 24 (1963) 909;
(b) L.L. Sun, Y. Cheng, G.F. Ji, J. At. Mol. Sci. 1 (2010) 143.
[30] W. Voigt, Lehrbuch der Kristallphysik, Taubner, Leipzig, 1928.
[31] A. Reuss, Z. Angew, Math. Mech. 9 (1929) 55.
[32] R. Hill, Proc. Soc. London A 65 (1952) 350.
[33] B. Kong, X.R. Chen, J.X. Yu, L.C. Cai, J. Alloys Compd. 509 (2011) 2611.
[34] X.L. Yuan, D.Q. Wei, X.R. Chen, Q.M. Zhang, Z.Z. Gong, J. Alloys Compd. 509 (2011) 769.
[35] J. Chang, X.R. Chen, D.Q. Wei, X.L. Yuan, Physica B 405 (2010) 3751.
[36] J. Chang, X.R. Chen, Y. Cheng, J. Zhu, Physica B 405 (2010) 529.
[37] G.V. Sin'ko, N.A. Smirnov, J. Phys.: Condens. Matter. 14 (2002) 6989.
[38] D.M. Teter, MRS Bull. 23 (1998) 22.
[39] S.F. Pugh, Philos. Mag. 45 (1954) 833.